The Astronomical Journal, 163:270 (14pp), 2022 June https://doi.org/10.3847/1538-3881/ac63d0

Origins of Chiral Life in Interstellar Molecular Clouds

Vlado Valković and Jasmina Obhođaš
Institute Ruđer Bošković, Experimental Physics Department, Laboratory for Nuclear Analytical Methods, Bijenička cesta 54, 10000 Zagreb, Croatia; valkovic@irb.hr, jobhodas@irb.hr
Received 2021 July 13; revised 2022 February 28; accepted 2022 March 28; published 2022 May 17

Abstract

The exploring of galactic chemical composition across the the Milky Way, and specifically across the solar neighborhood, provides insights into the chemical evolution of the universe. Since the formation of the first stars some hundred million years after the big bang (BB), heavier elements are synthesized in different stellar production processes at the expense of lighter elements. When the relative abundances of the life-forming elements evaluated for the Last Universal Common Ancestor (LUCA) are compared with the solar neighborhood stellar abundances, a striking similarity occurs. In this study, we tested the hypothesis that in some particular regions and at some particular time, the abundance curve of the first living matter and the universe coincided. Indeed, the best agreement between the two curves was obtained for $(4 \pm 1) \times 10^9$ yr after the BB, indicating the time of the origin of life. All organisms evolved on the Earth independently of place and time are leading to the LUCA and involve chiral molecules such as L amino acids and D sugars in fundamental life processes. The growing evidence from carbonaceous meteorites analysis shows an excess of L-type amino acids and D-type sugars, suggesting that the increase in L-type or D-type molecular chirality is the process that takes place in planetary and stellar forming systems, thus the life emerging from interstellar molecular clouds (IMCs) had to be chiral. Here we propose the spin-polarized proton–proton scattering as a potential physical process that takes place in IMCs environments and could lead to enrichment of L-type amino acids and D-type sugars.

Unified Astronomy Thesaurus concepts: Interstellar dust (836); Astrobiology (74); Galactic cosmic rays (567)

1. Introduction

To shed some light on the problems where and when life originated, we can hypothesize that life originated when the element abundance curve of the living matter and of the cosmic environment in which life originated coincided. This coincidence occurring at a particular space/time region of the universe can indicate when life originated, $T_{\rm origin}$. In $T_{\rm origin}$ the chemical abundance ratios of selected elements for a particular cosmic environment and living matter, corrected by the values of concentration factors, should be close to one. The life abundance curve that we have considered is of the only life we know: that on the planet Earth. In our considerations, we have taken the estimated essential elements abundances of the Last Universal Common Ancestor (LUCA; Chopra & Lineweaver 2015), ignoring the fact that we do not know the essential elements concentration factors for LUCA as we do not know his place of origin.

The interstellar medium (ISM) is a place of complex molecular synthesis. Many molecular species found on surfaces of comets, asteroids, meteorites, and interplanetary dust particles are used as life-forming molecules on the Earth (Ehrenfreund & Charnley 2000; Kwok 2004; Van Dishoeck 2014). When looking into the ISM as the possible environment of the origin of primitive life forms, our attention is on interstellar molecular clouds (IMCs). IMCs contain gas and small dust micron-sized particles, which play a critical role as a catalyst in the formation of interstellar complex molecules (Greenberg 2002; Cazaux et al. 2016; Minissale et al. 2016). The molecular species forming on the dust particle are easily desorbed into the gas phase of IMCs upon formation (Greenberg 2002; Cazaux et al. 2016; Minissale et al. 2016). These molecules are crucial for the initiation of life, and both, life-forming molecules and a primitive life form can participate in planetary condensation from the ISM, initiating planetary life and its subsequent evolution.

It is reasonable to suppose that life will not depend on resources that are scarce in its environment. The living matter needs only some chemical elements for its existence. Life, as we know, is (H–C–N–O) based and relies on the number of bulk elements (Na–Mg–P–S–Cl–K–Ca) for its existence. All existing organisms use a number of elements for providing proteins with unique coordination, catalytic, and electron transfer properties. This group of elements is called trace elements and it includes some (or all) of the following chemical elements: Li–B–F–Si–V–Cr–Mn–Fe–Co–Ni–Cu–Zn–As–Se–Mo–I–W. One can put in question the essentiality of some of these trace elements for life emerging. For example boron, which is depleted in the solar system, played an essential role in the process of life forming since its primary purpose has been to provide thermal and chemical stability in hostile environments (Scorei 2012). The fact that boron is not depleted in the ISM is yet another indication that life probably originated at a place different than Earth and the solar system.

There have been many attempts to elucidate the place and time of transition from abiotic to biotic forms that have eventually led to our existence. It is currently accepted that this transition has occurred on the Earth, probably after substantial delivery of the organic life building material during the heavy meteorite bombardment of the Earth some 3.9 Gy ago (Ehrenfreund et al. 2011). The emerging of life in places different from Earth is yet to be confirmed. Many studies are envisaging such scenarios (i.e., Loeb et al. 2016; McCabe & Lucas 2010; Sharov & Gordon 2017; Damer & Deamer 2020; Sasselov et al. 2020), but they all presume the existence of an Earth-like habitable zone for life to

emerge. Our approach is that environments that are capable of producing the life-forming building material, such are IMCs, are capable of producing the life itself, whereas the existence of a habitable zone such as Earth is necessary for life to evolve into more complex forms. Since there are no other life forms on the Earth that could lead to roots different from LUCA, and our research has shown that LUCA is apparently much older than the solar system, we can assume that life originated only once. Otherwise, there should be different types of organisms available on Earth governed by different physical, chemical, and biological processes. Anyway, the processes such are photosynthesis and chemosynthesis that enable primitive organisms to be to some extent independent from their environmental resources, are expected to be similar in extra-terrestrial and terrestrial bacteria (Sharov & Gordon 2017), thus resembling LUCA. These assumptions will be confirmed or disapproved after retrieving organisms from places other than Earth.

The chemical composition of the universe is changing because of its aging, while LUCA, assumed to be the child of its stellar environment, has passed the information of required essential elements as it was written in its genes at the time of its origin. By calculating the best agreement between essential elemental abundances in LUCA and corresponding elements of the solar neighborhood stars over their galactic evolution, we were able to find the time of LUCA's origin, presuming that the best agreement between the two curves is the most probable time of its origin.

1.1. Chirality Phenomenon

Together with a phenomenon of elements' essentiality, we should consider a closely related phenomenon of chirality. A living organism is an organized system of molecules having specific handedness, called chirality. Chiral molecules are designated D (dextrorotatory) or L (levorotatory) according to the right or left direction, respectively, in which the crystalline forms rotate polarized light. Biological polymers (e.g., nucleic acids and proteins), which function is determined by their shape, use almost exclusively D sugars and L amino acids. The exception is glycine as it has two (indistinguishable) hydrogen atoms attached to its alpha (central) carbon. Laboratory synthesis made from optically inactive starting materials yields racemic (1:1) mixtures of L and D isomers. Nineteen of the twenty amino acids used in the synthesis of proteins can exist as L or D enantiomorphs. Figure 1 shows examples of D and L amino acids and sugars.

As early as 1953, Frank (1953) has proposed the model of enantioselective autocatalysis where molecules maintain their own production while inhibiting the formation of the opposite enantiomer. This important model has shown that spontaneous asymmetric synthesis is a natural property of life. Joyce et al. (1984) found that template-directed reactions with a racemic mixture autocatalyze the replication of a polynucleotide of the same chirality, while the reactions with the opposite template were far less efficient. Moreover, it was noted that the incorporation of the monomers of the opposite chirality terminates the polymerization. Yin et al. (2015) have shown that chiral macroanions demonstrate chirality recognition behavior by forming a homogeneous blackberry structure via long-range electrostatic interactions between the individual enantiomers in their racemic solutions. Adding chiral coanions suppresses the self-assembly of one enantiomer while maintaining the assembly of the other one. However, for enantiomeric

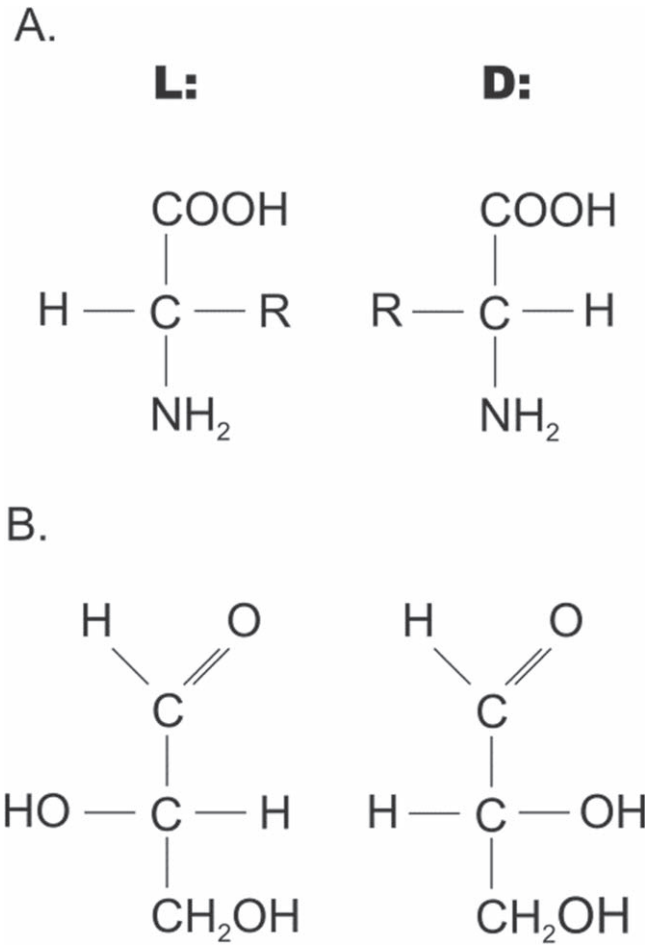

Figure 1. Two enantiomers (L-handed and D-handed) of (A) generic amino acid and (B) glyceraldehydes.

amplification to start, previously some physical or chemical process or their combination had to crack the symmetry between left-handed and right-handed molecules. There have been several suggestions, including (1) polarized light (De Marcellus et al. 2011; Garcia et al. 2019; MacDermott 2012), (2) optically active quartz, (Bonner et al. 1975; Vogl 2011), (3) natural radioactivity (MacDermott 2012), (4) cosmic rays (Boyd et al. 2018; Globus & Blandford 2020), and (5) nonenergetic mechanism (atom-addition surface reaction; Ioppolo et al. 2021). The small chiral bias produced in proposed processes is unlikely to lead to a homochiral state and some prebiotic mechanism is still required for enantiomeric amplification (Blackmond 2010).

We propose a new mechanism that might result in chirality excess, assuming that amino acids were synthesized on dust particles in interstellar space. This is the bombardment by cosmic rays of high-energy protons polarized in magnetic fields. Polarized proton cosmic rays preferentially destroy one isomer because of significant asymmetry in proton (in cosmic rays)—proton scattering (in amino acid/sugar) on the surface of ISM dust particles aligned by the magnetic fields. Such dust particle alignment has been observed for solar magnetic field and it is assumed to be the reason why the light scattered by cometary dust becomes circularly polarized (CP; Kolokolova et al. 2015). Actually, the most popular explanation of the CP formation is the scattering of light on aligned/irregular dust particles, or on the particles that contain homochiral molecules (Kolokolova & Nagdimunov 2014).

Considering the chemical composition of dust in interstellar molecular clouds (Zhukovska et al. 2008) and recent findings in the field of prebiotic solid-state chemistry (Oba et al. 2019; Stolar et al. 2020), which show that the evolution from molecular clouds to stars and planets provides a suitable environment for nucleobase synthesis in space, we can hypothesize that life arose chiral because originated in the IMCs with the critical role of dust particles, magnetic fields, and exposure to cosmic rays. The arguments supporting the hypothesis are put forward based on numerous astrophysical observations and physics laws.

2. Methods

The elemental abundances for the solar neighborhood have been obtained from the experimental values summarized in (Kobayashi et al. 2020). The elemental abundances for LUCA have been taken from (Chopra & Lineweaver 2015) and expressed relative to iron. The agreement between life essential bulk and trace elements in LUCA and the solar neighborhood as a function of metallicity [Fe/H] have been calculated for different [Fe/H] values corresponding to different times, T values, according to the age-[Fe/H] model presented in (Kobayashi et al. 2020). Only those essential elements available for the evaluation of the solar neighborhood chemical evolution presented in (Kobayashi et al. 2020) have been selected (C, N, O, Na, Mg, Al, Si, P, S, K, Ca, V, Cr, Mn, Co, Ni, Cu, Zn, and Mo).

Two approaches have been used to estimate the time of the life origin, $T_{\rm origin}$. First, we calculated the minimum of χ^2 (best agreement) as defined by

$$X^2 = \frac{1}{N}\sum_{\rm i=1}^{\rm N}({\rm C_{i,LUCA}} - {\rm C_{i,SN}})^2/{\rm C_{i,SN}},$$

where C_i is the abundance of essential element i in LUCA and in the solar neighborhood (SN) where LUCA originated. In the second approach, we have calculated the maximum coefficient of determination (R^2), i.e., the percentage of the variance explained by the linear regression model between logarithmic values of abundances of essential elements in LUCA and the environment of its origin. The χ^2 and R^2 have been calculated for 19 essential elements (as mentioned above), and χ^2 also for the subgroup of trace elements (V, Cr, Mn, Co, Ni, Cu, and Zn). Row data used for χ^2 and R^2 calculations are presented in the Appendix. Uncertainties for χ^2 and R^2 are expressed as a standard deviation of a mean and were calculated by bootstrapping using software Resampling Stats Addin for Excel of The Institute for Statistics Education, An Elder Research Company, Arlington, Virginia, United States.

3. Results and Discussion

3.1. The Estimation of T_{origin}

For the determination of the time of the life origin, $T_{\rm origin}$, we have to consider only well-characterized cosmic environments such as the solar neighborhood, for which the elemental abundance curves for elements of our interest could be constructed from the measured data or existing models. Recently, Kobayashi et al. (2020) constructed Galactic Chemical Evolution models for the solar neighborhood. Their calculations result in concentration values for all stable elements from ^{12}C to ^{238} U, based on theoretical nucleosynthesis yields and event rates of all nucleosynthesis processes involved in elemental synthesis as a function of time and environment. The basic equations of chemical evolution are described by Kobayashi et al. (2000).

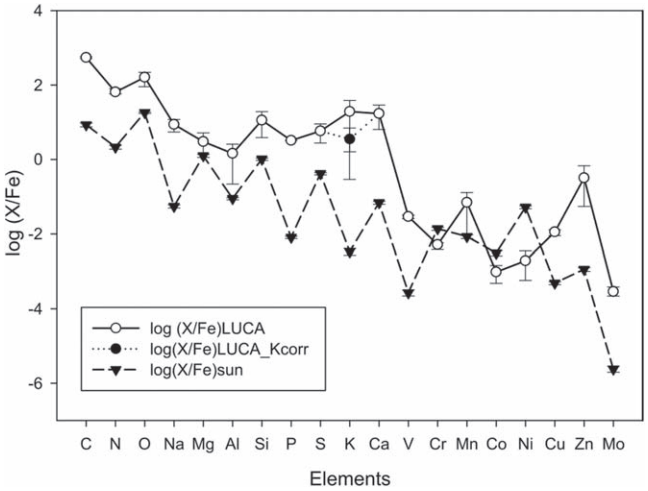

Figure 2. The abundance curves of LUCA (after Chopra & Lineweaver 2015) and the present Sun (after Asplund et al. 2009) for selected essential elements. The closed circle presents the correction for the abundance of potassium measured in *Bacillus subtilis* for the 100 nT magnetic field (Obhođaš et al. 2021).

Considering the life abundance curve, it is the common understanding that all organisms on the tree of life have a common ancestor, i.e., the tree is rooted in the LUCA. Therefore, to establish an average elemental composition of life one needs to estimate the relative abundance of elements in LUCA. One such effort has been undertaken by Chopra et al. (2009) and Chopra & Lineweaver (2015). They considered the elemental composition of eukaryotic, bacterial, and archaeal species, as well as the phylogenetic relationship between them. Although the idea of LUCA or the progenitor is the most important for the study of early evolution and life's origin, the information about when, where, and how LUCA originated is still lacking. Namely, considerable time and extinct organisms might have existed between the origin of life and the root of the tree, as defined by extant organisms (Cornish-Bowden & Cárdenas 2017). All these considerations are done by assuming that Earth's present-day three existing domains of life define the LUCA's capabilities and characteristics. However, as pointed out by Cockell (2015), we cannot be sure that there were not domains that went extinct early in the history of life and took with them crucial information.

Figure 2 presents concentrations of selected essential elements relative to iron in LUCA, compared to the same for the present Sun (Asplund et al. 2009). It has been recently shown by Obhođaš et al. (2021) that preconcentration factors can be different in very low magnetic fields. *Bacillus subtilis* grown in magnetic fields of 100 nT, which are intensities found in IMCs (Crutcher 2012), required 5.5 times less potassium compared to the control culture growing in the Earth's magnetic field. Magnetic, as well as gravitational fields, are orders of magnitude weaker in IMCs compared to the Earth. Thus, the abundances derived for LUCA may be severely misleading. If potassium abundance in LUCA is corrected by factor 5.5 inferred from the experiment with the *Bacillus subtilis* grown in the magnetic field of 100 nT (Obhođaš et al. 2021), the LUCA abundance curve resembles the Sun abundance curve more closely. The essential element concentration factors of primitive life forms for intensities of magnetic and

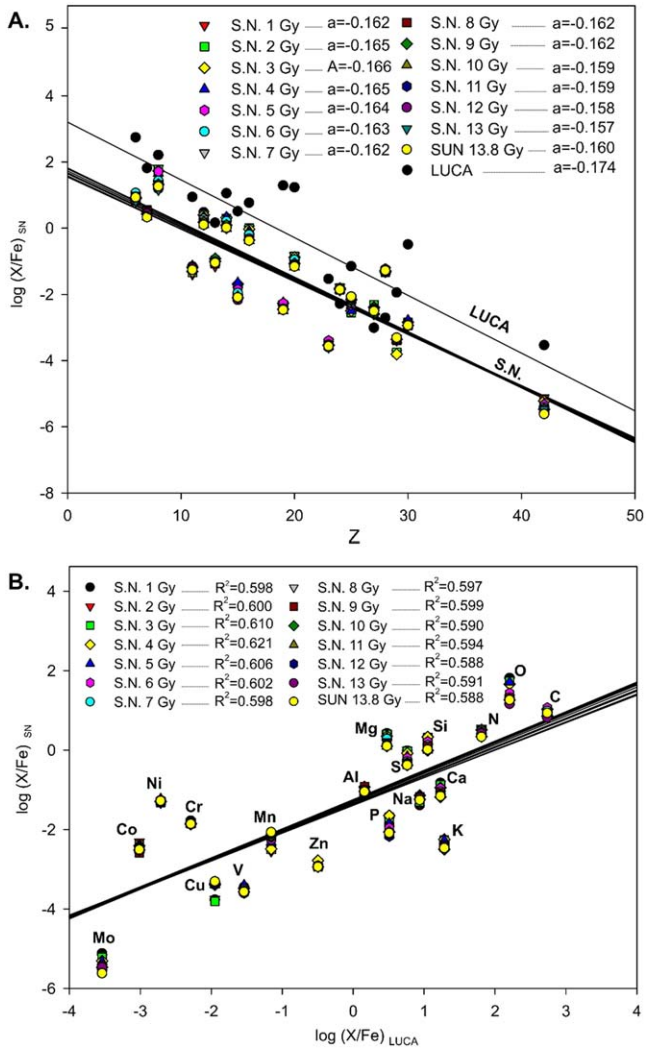

Figure 3. (A) The comparison of a set of 19 essential elements abundances in LUCA, present Sun, and in stars of the solar neighborhood over their chemical evolution, which is evident as changes in linear regression slope coefficients, *a*. (B) The linear regression analyses between 19 essential elements abundances in LUCA and stars of the solar neighborhood over their evolution, including the present Sun.

gravitational fields found in IMCs will be systematically studied in our future research.

Figure 3(a) shows the comparison of abundances for a set of 19 elements (C, N, O, Na, Mg, Al, Si, P, S, K, Ca, V, Cr, Mn, Co, Ni, Cu, Zn, and Mo) in LUCA, present Sun, and stars of the solar neighborhood over their chemical evolution, whereas their chemical evolution is being evident as changes in linear regression slope coefficients. Figure 3(b) presents the linear regression analyses between the set of 19 elements' abundances in LUCA and stars of the solar neighborhood over their evolution, including the present Sun. The complete match between LUCA and his solar environment would yield $R^2 = 1$, but this is hardly expected because highly volatile elements such are C, O, and N are not completely preserved on the IMCs dust particles, and elementals abundances derived for LUCA are to some extent modified by the Earth environment.

Figures 4(a) and (c) present the χ^2 and R^2 estimates, respectively, for a set of 19 elements' abundances in the solar neighborhood stars over their galactic evolution, and those inferred for LUCA. The χ^2 estimates calculated for abundances

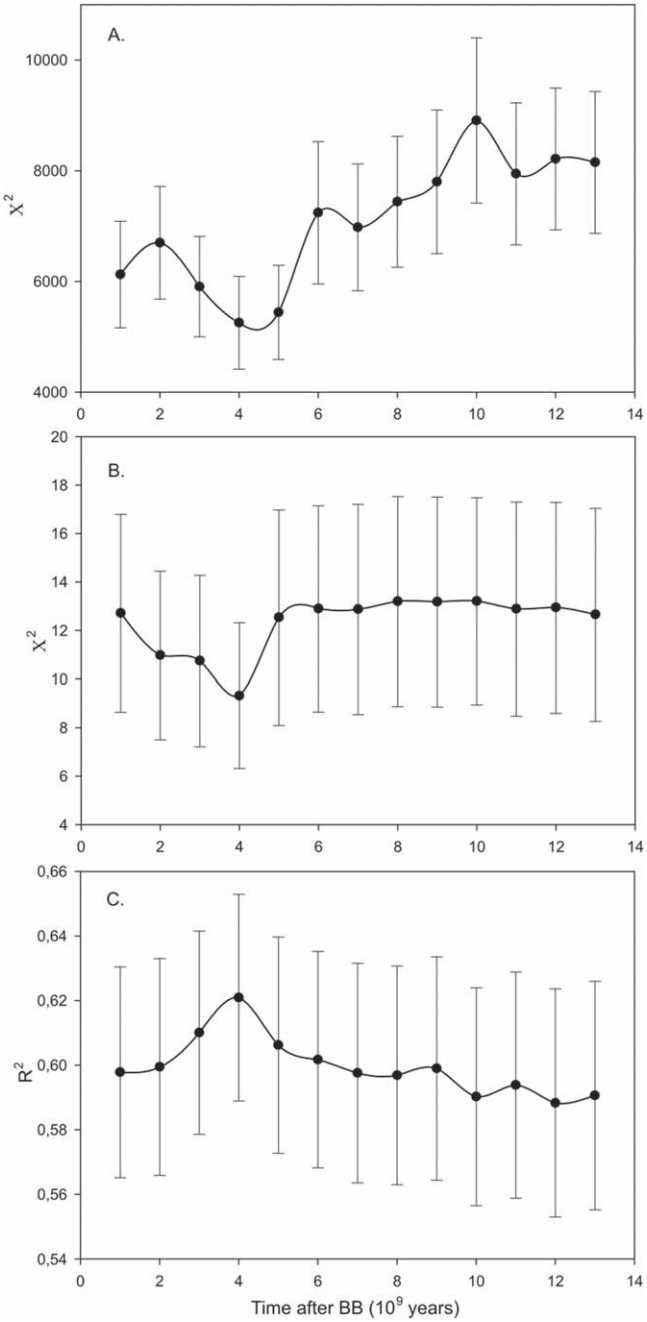

Figure 4. The χ^2 and R^2 estimates for the solar neighborhood data and LUCA. 19 essential elements (A) and (C), and the subgroup of seven essential trace elements (B) have been taken into consideration. The uncertainties shown are the standard error of the mean calculated by a bootstrapping method.

of selected 7 trace elements (V, Cr, Mn, Co, Ni, Cu, and Zn) are shown in Figure 4(b). In all cases, T_{origin} of (3–5) $\times 10^9$ yr after the big bang (BB) is observed ($(4 \pm 1) \times 10^9$ after BB). However, the large uncertainty of age determination derived from the age—[Fe/H] metallicity model, as well as uncertainties derived by extrapolation and interpolation of solar neighborhood abundances of elements from graphical diagrams presented in Kobayashi et al. (2020), should be taken into account. On the other hand, the corrections for concentration factors in LUCA would shift the χ^2 and R^2 curves presumably toward the better agreement between two data sets (those for LUCA and the abundances of elements in stars of the solar neighborhood), but it would not change the shape of the χ^2 and R^2 curves. For example, the correction for potassium

in LUCA for a factor of 5.5 (Obhođaš et al. 2021) shifts up the R^2 estimates for 0.035 (i.e., 3.5% better agreement was observed between abundance curves for LUCA and stars of the solar neighborhood throughout their chemical evolution).

A different approach for estimation of origin of life based on extrapolation of the genetic complexity of organisms back to just one base pair has yield $T_{\rm origin} = (9.7 \pm 2.5) \times 10^9$ ago (or $(4.1 \pm 2.5) \times 10^9$ after BB; Sharov & Gordon 2017), which almost exactly match our estimation of $T_{\rm origin} = (9.8 \pm 1) \times 10^9$ ago (or $(4.0 \pm 1.0) \times 10^9$ after BB). Our estimation of $T_{\rm origin}$ lower boundary of 3×10^9 yr after BB can be further supported by the trends in dust composition as presented for the solar neighborhood by Zhukovska et al. (2008). The evolution of the dust composition is closely related to the stellar injection of the elements in ISM and therefore to the galactic chemical evolution, although slight differences can be observed with respect to volatile elements. In particular, one should pay attention to the C/O ratios found in ISM dust particles, stars of the solar neighborhood, and our planet, compared to the C/O ratio inferred for LUCA. Throughout the galactic evolution, the C/O ratio is <1 for most stars of the solar neighborhood (see Appendix). The C/O ratio for the Earth's crust is also less than 1 (Demayo 1983). Yet, the C/O ratio for LUCA is above 1 and also for ISM dust particles in the solar neighborhood starting from 3×10^9 yr after BB (Zhukovska et al. 2008) suggesting that life most probably originated on the carbonaceous dust particles of IMCs. Furthermore, the huge star formation rate in our galaxy for the first 3×10^9 yr after BB in the bulge and thick disk regions (Kobayashi et al. 2020) probably excludes these regions as possible places for life to emerge, although they might have reached the right distribution of elemental abundances for the emergence of life earlier than the solar neighborhood and halo. However, if life was not able to be sustained in such restless systems, it may have been propagated into ISM during the supernova explosion to potentially seed the more friendly habitable zones such as our solar system.

3.2. IMCs—The Environment Where Life Might Have Originated

ISM is composed primarily of hydrogen in its atomic, ionic, or molecular form and dust particles. Two forms of ISM are distinguished: interstellar diffuse clouds and IMCs. Interstellar diffuse clouds consist of atomic hydrogen. They can have kinetic temperatures of 50–100 K and a density of hydrogen atoms below 300 per cm^3. Molecular hydrogen is the main component of IMCs, which are of interest to this study because they are the place where the complex organic molecules are formed on the dust particles which they contain. IMCs are at kinetic energies as low as 20–10 K, they can have any density above 300 per cm^3, and at critical densities collapse to form stars and planetary systems. However, the dust in ISM is at a lower temperature than gas. In diffuse interstellar clouds, the ultraviolet radiation heats the dust to 15 K, while the IMCs dust is shielded and the temperature may be as low as 5–10 K (Greenberg 1971, 2002; Greenberg & Li 1997).

The recent laboratory achievements suggest that solid-state chemistry was crucial in the synthesis of RNA and DNA building blocks and their polymerization, both on early Earth (Forsythe et al. 2015; Becker et al. 2018; Bolm et al. 2018; Lamour et al. 2019) and in ISM (Oba et al. 2019). Oba et al. (2019) reported the simultaneous detection of all three pyrimidine (cytosine, uracil, and thymine) and three purine nucleobases (adenine, xanthine, and hypoxanthine) in interstellar ice analogs examined in environmental conditions simulating those in IMCs. Stolar et al. (2020) have achieved self-assembly of DNA by heating solid nucleobase mixtures.

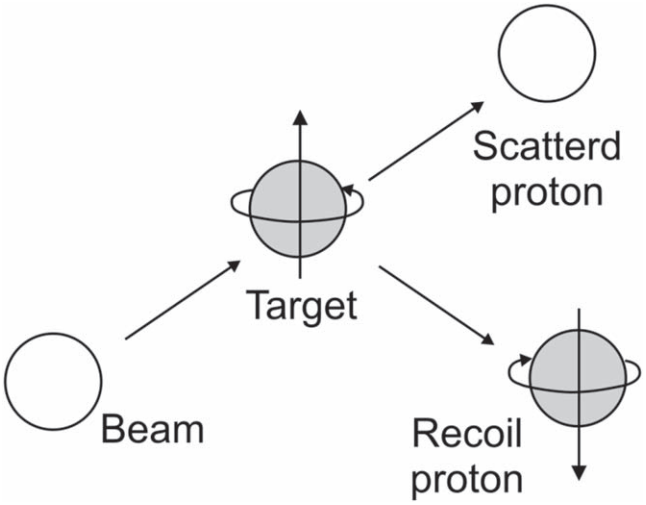

Figure 5. The elastic scattering process. The asymmetry arises from the interference between a spin-flip (coulomb) and spin nonflip (nuclear) amplitude.

The findings of Obhođaš et al. (2021) demonstrated that magnetic fields below 400 nT significantly enhance the growth of *Bacillus subtilis* compared to controls growing in the Earth's magnetic field. This might suggest that microorganisms favor extremely low magnetic fields. The Earth's magnetic field of the approximately same intensity as presently (between 33 μT at the magnetic equator, and 67 μT at the magnetic poles), formed 4.2×10^9 yr ago, almost immediately after the lunar-forming giant impact (Tarduno et al. 2020). Moreover, it has been shown that microorganisms in a very similar way favor microgravity (Horneck et al. 2010). These findings of microorganisms favoring the low magnetic and gravitational fields, evident as 10 times increase in their multiplication rate, strengthen the assumption that life originated in IMCs, where maximum magnetic field intensities are ~100 nT (Crutcher 2012) and strong gravitational fields are not yet formed.

3.3. Preferential Destruction of Enantiomers by Spin-polarized Cosmic-Ray Protons

The sources of accelerated protons that might collide with individual atoms or dust particles in IMCs are the primary cosmic rays irradiated by stars, black holes, or the BB itself. The primary cosmic rays consist of 95% protons, 4% of helium, and 1% of heavier elements up to iron. Their energies could be enormous, from 10^9 eV (1 GeV) up to 10^{20} eV (10^8 TeV; Kliewer 1995). Since they are charged (otherwise they cannot be accelerated), they can be polarized by magnetic fields on their path through the IMCs. Polarized protons colliding with dust particles might be elastically scattered in spin-polarized proton–proton (p-p) reaction as shown in Figure 5. Either proton (beam or target) can be polarized.

One of the main characteristics of the p-p elastic scattering reaction in the energy range of primary cosmic-ray protons is the asymmetry between the number of scatterings on the left versus on the right, which can be above 5% (Akchurin et al. 1993;

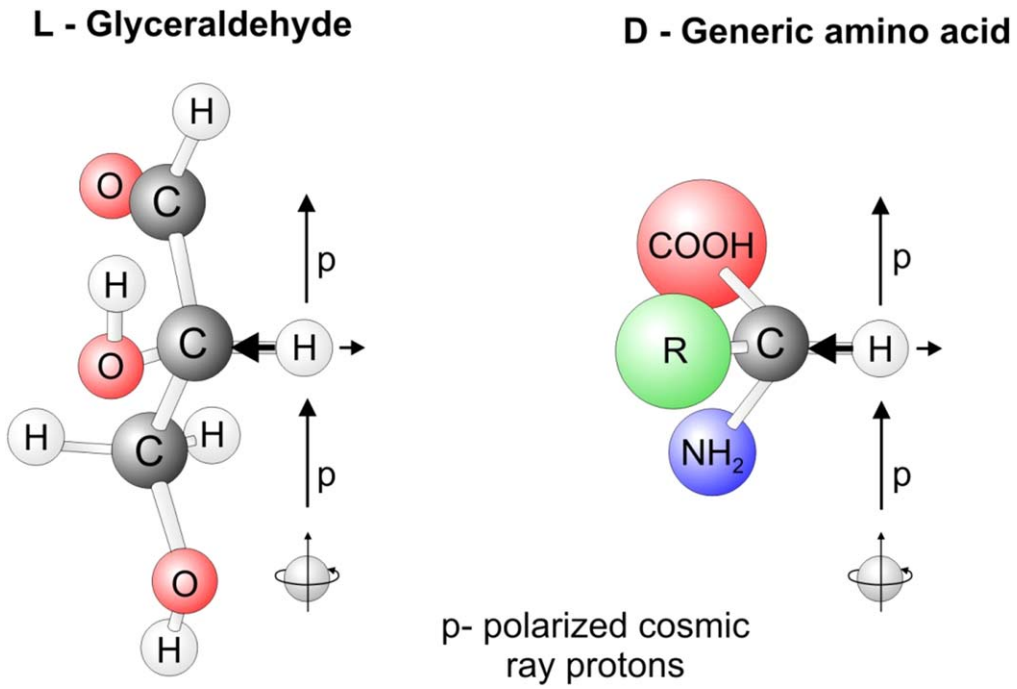

Figure 6. Schematic presentation of the process of preferential destruction of L sugars and D amino acids. The bolded arrow presents the asymmetry in scattering which can be above 5%.

Bazilevsky et al. 2011; Bravar et al. 2005; Okada et al. 2008; Adamczyk et al. 2013). Polarization-induced asymmetry produced in p-p scattering has been observed even at low energies of 30 and 50 MeV (Batty et al. 1963). The spin-polarized p-p reaction has been overlooked in the scientific literature as the possible cause of prebiotic molecular chirality. Sugars and amino acids involved in life fundamental processes of all taxa in the tree of life are exclusively single enantiomers, although both enantiomers have a similar probability of their formation in an achiral environment (Prelog 2006). Enantiomer's selection is critical for molecular interaction and replication processes, thus, it is crucial for understanding the origin of life.

Polarization of IMCs dust grains might be probed by observing ultraviolet (UV) to infrared (IR) polarization (Andersson et al. 2015). The observed UV-IR electromagnetic spectrum polarization in IMCs may have two possible sources that could be involved alone or combined. (i) The first process arises from dust grains which consist of silicates, amorphous carbon, and small graphite particles of asymmetric shape that have a tendency to align with the magnetic field. Only a limited number of relatively large grain sizes ($\sim$0.01–1 μm) contribute to the polarization. These particles might aggregate in the dark cold parts of IMCs (Andersson et al. 2015; Greenberg 2002). The situation corresponds to a polarized target in the p-p elastic scattering process. (ii) Alternatively, polarized beam interaction could be considered. High-energy polarized protons in cosmic rays may be able to preferentially destroy one isomer on the dust particle surface because of significant asymmetry in proton (in cosmic rays)—proton (placed next to chirality center in amino acid or sugar) scattering. See Figure 6. for the schematic presentation of the process leading to preferential destruction of L sugars and D amino acids.

Preferential destruction of one enantiomer leads to a disbalance of molecules available from the primordial reservoir of IMCs, which would almost certainly result in an extreme bias of enantiomers selection by emerging life (Blackmond 2010; McGuire & Carroll 2016). Analysis of amino acids in meteoritic samples, such as the one that hit Murchison, Australia, shows an excess of left-handed enantiomers of up to 10% suggesting that such an enantiomeric excess has been generated before the Earth's formation (McGuire & Carroll 2016). The process shown in Figure 6 could have generated an enantiomeric excess in left-handed amino acids and right-handed sugars, thus linking the origins of life's enantiomeric bias to IMCs. Since the life in the universe emerged probably long before the occurrence of our solar system as suggested by a comparison of life and stellar elements abundance curves, it is reasonable to assume that dust that formed our solar system already contained life in some primitive form.

4. Conclusions

We have presented numerous examples of observations, experiments, and theoretical considerations, which we have used to synthesize our hypothesis concerning the origin of life on interstellar dust particles. The universe was born only with plenty of hydrogen isotopes, some helium, and lithium, while all other elements were formed as the universe aged through star formation processes, their lives, and deaths, which resulted in dust clouds as a birthplace of a new generation of stars. During this process of the universe aging, the chemical element abundance curve has been changing in such a manner that at the time $T_{\rm origin}$ coincided with the abundance curve of living matter. Our hypothesis defines $T_{\rm origin}$ as a time when conditions were right for life to originate in the primitive form.

Exposure to cosmic rays and magnetic fields as well as physical, chemical, and biological processes made life chiral. Our preliminary considerations of the solar neighborhood as a part of the Milky Way galaxy indicate period of $(4 \pm 1) \times 10^9$ yr after BB for the origin of life on the carbonaceous dust particles in the IMCs of the solar neighborhood. The same could be expected for similar zones in other spiral galaxies. Emerged life could have survived the planet formation processes to evolve in habitable

zones of stars. Since all organisms on Earth seem to converge in LUCA, and our study has shown that LUCA is much older than the solar system, it could be assumed that life emerged only once in the history of the universe. This assumption is yet to be confirmed after retrieving the organisms from places different from Earth. During the seedings of habitable zones along the universe, the primitive organisms have had to adjust to a certain extent their need for essential elements to new environments. This should be seen in concentration factors dependence on environment's properties, in particular, due to organisms' adaptation to different magnetic and gravitational fields, and the availability of essential elements.

Some of the ideas presented in this paper have been discussed in a great many details in the book Origins of Life–Musings from Nuclear Physics, Astrophysics and Astrobiology (Valkovic 2022).

Author Contributions:

V.V. initiated and designed the research, J.O. analyzed data and both authors contributed to the paper writing.

Competing Interest Statement:

The authors have no competing interests.

Appendix
Elemental Abundances for LUCA, Present Sun, and Solar Neighborhood over Galactic Chemical Evolution

Table A1
Estimated Essential Elements Concentrations Relative to Fe for LUCA (Chopra & Lineweaver 2015)

Element	Z	LUCA (Fe=1)	Minimum	Maximum
H	1	483.87	274.193	629.031
B	5	0.516128	0.451612	0.580644
C	6	548.386	516.128	580.644
N	7	64.516	58.0644	80.645
O	8	161.29	90.3224	219.3544
F	9	0.01870964	0.01870964	0.01870964
Na	11	8.70966	5.48386	11.93546
Mg	12	2.999994	1.354836	5.16128
Al	13	1.45161	0.2193544	2.58064
Si	14	11.2903	3.87096	19.3548
P	15	3.2258	3.2258	3.2258
S	16	5.80644	2.774188	9.03224
Cl	17	25.8064	8.70966	45.1612
K	19	19.3548	1.6129	38.7096
Ca	20	17.09674	6.4516	29.0322
V	23	0.0290322	0.0258064	0.032258
Cr	24	0.00516128	0.00387096	0.00580644
Mn	25	0.0741934	0.0096774	0.129032
Fe	26	0.999998	0.354838	1.29032
Co	27	0.00096774	0.00048387	0.00145161
Ni	28	0.00193548	0.00058064	0.00354838
Cu	29	0.0112903	0.00903224	0.0129032
Zn	30	0.32258	0.0548386	0.677418
As	33	0.00016129	7.0968E-06	0.00029032
Se	34	5.80644E-05	6.7742E-07	7.4193E-05
Mo	42	0.000290322	0.00021935	0.0003871
I	53	0.000548386	0.00054839	0.00054839
W	74	0.000048387	4.8387E-05	4.8387E-05

Table A2
Concentrations of Selected Elements in Present Sun (Asplund et al. 2009)

Element	Z	Photosphere (log)	Uncert. (+/−)	log(X/Fe)	(X/Fe)
H	1	12			
B	5				
C	6	8.43	0.05	0.93	8.51138
N	7	7.83	0.05	0.33	2.137962
O	8	8.76	0.02	1.26	18.19701
F	9				
Na	11	6.24	0.04	−1.26	0.054954
Mg	12	7.6	0.04	0.1	1.258925
Al	13	6.45	0.03	−1.05	0.089125
Si	14	7.51	0.03	0.01	1.023293
P	15	5.41	0.03	−2.09	0.008128
S	16	7.12	0.03	−0.38	0.416869
Cl	17				
K	19	5.03	0.09	−2.47	0.003388
Ca	20	6.34	0.04	−1.16	0.069183
V	23	3.93	0.08	−3.57	0.000269
Cr (III)	24	5.64	0.04	−1.86	0.013804
Mn	25	5.43	0.05	−2.07	0.008511
Fe	26	7.5	0.04	0	1
Co	27	4.99	0.07	−2.51	0.00309
Ni	28	6.22	0.04	−1.28	0.052481
Cu	29	4.19	0.04	−3.31	0.00049
Zn	30	4.56	0.05	−2.94	0.001148
As	33				
Se	34				
Mo	42	1.88	0.08	−5.62	2.4E-06
I	53				
W	74				

Note. Only those essential elements for LUCA that were also evaluated for stars of the solar neighborhood over their chemical evolution (Kobayashi et al. 2020) are shown.

Table A3
Geometric Median and Range of Selected Elements' Abundances in Stars of the Solar Neighborhood Relative to Sun, on a Logarithmic Scale, over First 5×10^9 Years following the BB (Kobayashi et al. 2020)

After BB	1 Gy		2 Gy		3 Gy		4 Gy		5 Gy	
Metallicity [Fe/H]	−1.555		−1.255		−1.07		−0.94		−0.68	
	[X/Fe]	Range (+/−)	[X/Fe]	Range (+/−)	[X/Fe]	Range (+/−)	[X/Fe]	Range (+/−)	[X/Fe]	Range (+/−)
Z										
1										
5										
6	−0.03	0.3	−0.1	0.2	−0.03	0.25	0.1	0.3	0.1	0.2
7	0.02	0.32	0.22	0.18	0.18	0.14	0.01	0.19	0.15	0.33
8	0.55	0.2	0.51	0.13	0.47	0.28	0.4	0.21	0.45	0.21
9										
11	−0.13	0.26	−0.08	0.22	−0.05	0.23	0.12	0.02	0.08	0.13
12	0.32	0.17	0.31	0.13	0.3	0.13	0.25	0.16	0.21	0.21
13	−0.1	0.21	−0.02	0.21	0.05	0.22	0.12	0.2	0.12	0.11
14	0.24	0.19	0.28	0.16	0.31	0.15	0.32	0.13	0.2	0.16
15	0.22	0.58	0.32	0.42	0.4	0.29	0.44	0.2	0.24	0.25
16	0.36	0.15	0.38	0.11	0.35	0.16	0.3	0.12	0.22	0.16
17										
19	0.18	0.16	0.15	0.11	0.2	0.11	0.22	0.11	0.2	0.25
20	0.33	0.12	0.31	0.04	0.28	0.1	0.21	0.15	0.12	0.17
23	0.12	0.23	0.06	0.18	0.04	0.18	0.09	0.27	0.17	0.23
24	0.08	0.08	0.05	0.06	0.04	0.06	0.02	0.06	0.01	0.08
25	−0.43	0.15	−0.48	0.07	−0.43	0.14	−0.42	0.09	−0.25	0.16
26										
27	0.05	0.12	0.2	0.06	0.12	0.19	0.1	0.1	0.1	0.08
28	0	0.22	−0.05	0.15	−0.04	0.13	−0.02	0.18	0.05	0.14
29	−0.46	0.27	−0.44	0.07	−0.5	0.33	−0.08	0.12	−0.01	0.15
30	0.02	0.17	0.09	0.23	0.1	0.14	0.16	0.21	0.02	0.14
33										
34										
42	0.5	0.3	0.4	0.4	0.4	0.38	0.31	0.26	0.29	0.26
53										
74										

Table A4
Geometric Median and Range of Selected Elements' Abundances in Stars of the Solar Neighborhood Relative to Sun, on a Logarithmic Scale, from 6×10^9 to 10×10^9 Years following the BB (Kobayashi et al. 2020)

After BB	6 Gy		7 Gy		8 Gy		9 Gy		10 Gy	
Metallicity [Fe/H]	−0.45		−0.3		−0.19		−0.1		−0.025	
	[X/Fe]	Range (+/−)	[X/Fe]	Range (+/−)	[X/Fe]	Range (+/−)	[X/Fe]	Range (+/−)	[X/Fe]	Range (+/−)
Z										
1										
5										
6	0.13	0.1	0.05	0.1	0.03	0.1	0	0.09	−0.08	0.07
7	0.09	0.01	0.17	0.29	0.18	0.26	0.1	0.41	0.18	0.18
8	0.17	0.22	0.05	0.1	0.05	0.11	0.06	0.12	0	0.12
9										
11	0.1	0.03	0.05	0.03	0.03	0.05	0.08	0.1	0.02	0.1
12	0.18	0.2	0.18	0.15	0.08	0.14	0.08	0.14	0	0.1
13	0.02	0.1	0.02	0.11	0.03	0.12	0.13	0.1	0.01	0.14
14	0.2	0.14	0.11	0.12	0.08	0.11	0.08	0.1	−0.02	0.11
15	0.13	0.28	0	0.4	−0.02	0.24	−0.01	0.23	0.03	0.21
16	0.18	0.15	0.09	0.26	0.04	0.16	0.02	0.19	0	0.18
17										
19	0.02	0.11	0.07	0.16	0.04	0.15	0.02	0.09	−0.03	0.12
20	0.2	0.21	0.11	0.14	0.05	0.1	0.09	0.11	−0.02	0.08
23	0.05	0.16	0.06	0.18	0.02	0.15	0.03	0.15	0	0.1
24	0	0.09	−0.01	0.09	0	0.07	0.01	0.07	−0.01	0.9
25	−0.18	0.13	−0.12	0.1	−0.11	-0.25	−0.09	0.09	−0.08	0.07
26										
27	0.05	0.14	0.03	0.13	−0.02	0.1	−0.08	0.11	−0.01	0.06
28	0	0.09	0	0.09	−0.01	0.07	−0.01	0.07	−0.01	0.07
29	−0.07	0.1	−0.08	0.11	−0.08	0.12	−0.05	0.1	−0.05	0.1
30	0.01	0.18	0.01	0.18	0	0.1	0	0.1	0	0.15
33										
34										
42	0.2	0.17	0.15	0.07	0.15	0.07	0.15	0.07	0.15	0.07
53										
74										

Table A5
Geometric Median and Range of Selected Elements' Abundances in Stars of the Solar Neighborhood Relative to Sun, on a Logarithmic Scale, from 11×10^9 to 13×10^9 Yr following the BB (Kobayashi et al. 2020)

After BB	11 Gy		12 Gy		13 Gy	
Metallicity [Fe/H]	0.03		0.085		0.14	
	[X/Fe]	Range (+/−)	[X/Fe]	Range (+/−)	[X/Fe]	Range (+/−)
Z						
1						
5						
6	−0.05	0.13	−0.1	0.21	−0.11	0.22
7	0.13	0.21	0.11	0.21	0.09	0.1
8	−0.05	0.17	−0.07	0.15	−0.1	0.12
9						
11	0.06	0.15	0.06	0.15	0.05	0.08
12	0	0.12	0	0.12	0.03	0.11
13	−0.01	0.15	0.03	0.07	0.04	0.11
14	−0.01	0.12	0	0.1	−0.01	0.09
15	−0.04	0.1	−0.08	0.09	−0.02	0.2
16	0.04	0.15	0.06	0.18	0.03	0.21
17						
19	0.03	0.17	0.03	0.17	0.04	0.13
20	0.04	0.09	0.04	0.09	0.03	0.08
23	0.02	0.12	−0.03	0.06	−0.03	0.02
24	−0.01	0.09	0	0.1	−0.01	0.12
25	−0.01	0.14	−0.03	0.07	−0.03	0.11
26						
27	0	0.04	0.02	0.05	−0.01	0.01
28	−0.01	0.06	0	0.07	0.01	0.09
29	−0.08	0.17	−0.06	0.17	−0.01	0.1
30	0.01	0.15	0.01	0.15	0.02	0.15
33						
34						
42	0.15	0.07	0.15	0.07	0.15	0.07
53						
74						

Table A6

Geometric Median and Range of Selected Elements' Abundances in LUCA and Stars of the Solar Neighborhood, Relative to Fe, Over First 5×10^9 yr Following the BB (Kobayashi et al. 2020)

	$(X/Fe)_{LUCA}$	$(X/Fe)_{SN}$ 1 Gy	$(X/Fe)_{SN}$ 2 Gy	$(X/Fe)_{SN.}$ 3 Gy	$(X/Fe)_{SN}$ 4 Gy	$(X/Fe)_{SN}$ 5 Gy
Z						
1						
5						
6	548.39	7.943282347	6.76083	7.943282	10.71519	10.71519
7	64.52		3.548134	3.235937	2.187762	3.019952
8	161.29	64.5654229	58.88437	53.70318	45.70882	51.28614
9						
11	8.71	0.040738028	0.045709	0.048978	0.072444	0.066069
12	3	2.630267992	2.570396	2.511886	2.238721	2.041738
13	1.45	0.070794578	0.085114	0.1	0.11749	0.11749
14	11.29	1.77827941	1.949845	2.089296	2.137962	1.62181
15	3.23	0.013489629	0.016982	0.020417	0.022387	0.014125
16	5.81	0.954992586	1	0.933254	0.831764	0.691831
17						
19	19.35	0.005128614	0.004786	0.00537	0.005623	0.00537
20	17.1	0.147910839	0.141254	0.131826	0.112202	0.091201
23	0.029032	0.000354813	0.000309	0.000295	0.000331	0.000398
24	0.005161	0.016595869	0.015488	0.015136	0.014454	0.014125
25	0.07	0.003162278	0.002818	0.003162	0.003236	0.004786
26						
27	0.000968	0.003467369	0.004898	0.004074	0.00389	0.00389
28	0.00194	0.052480746	0.046774	0.047863	0.050119	0.058884
29	0.01129	0.000169824	0.000178	0.000155	0.000407	0.000479
30	0.32	0.001202264	0.001413	0.001445	0.00166	0.001202
33						
34						
42	2.90E-04	7.58578E-06	6.03E-06	6.03E-06	4.9E-06	4.68E-06
53						
74						

Table A7
Geometric Median and Range of Selected Elements' Abundances in LUCA and Stars of the Solar Neighborhood, Relative to Fe, from 6×10^9 to 10×10^9 Years following the BB (Kobayashi et al. 2020)

	$(X/Fe)_{SN}$ 6 Gy	$(X/Fe)_{SN}$ 7 Gy	$(X/Fe)_{SN}$ 8 Gy	$(X/Fe)_{SN}$ 9 Gy	$(X/Fe)_{SN}$ 10 Gy
Z					
1					
5					
6	11.48154	9.549926	9.120108	8.51138	7.079458
7	2.630268	3.162278	3.235937	2.691535	3.235937
8	26.91535	20.41738	20.41738	20.89296	18.19701
9					
11	0.069183	0.06166	0.058884	0.066069	0.057544
12	1.905461	1.905461	1.513561	1.513561	1.258925
13	0.093325	0.093325	0.095499	0.120226	0.091201
14	1.62181	1.318257	1.230269	1.230269	0.977237
15	0.010965	0.008128	0.007762	0.007943	0.00871
16	0.630957	0.512861	0.457088	0.436516	0.416869
17					
19	0.003548	0.003981	0.003715	0.003548	0.003162
20	0.109648	0.089125	0.077625	0.085114	0.066069
23	0.000302	0.000309	0.000282	0.000288	0.000269
24	0.013804	0.01349	0.013804	0.014125	0.01349
25	0.005623	0.006457	0.006607	0.006918	0.007079
26					
27	0.003467	0.003311	0.002951	0.00257	0.00302
28	0.052481	0.052481	0.051286	0.051286	0.051286
29	0.000417	0.000407	0.000407	0.000437	0.000437
30	0.001175	0.001175	0.001148	0.001148	0.001148
33					
34					
42	3.8E-06	3.39E-06	3.39E-06	3.39E-06	3.39E-06
53					
74					

Table A8
Geometric Median and Range of Selected Elements' Abundances in LUCA and Stars of the Solar Neighborhood, including Sun, Relative to Fe, from 10×10^9 to 13×10^9 Years following the BB (Kobayashi et al. 2020)

	$(X/Fe)_{SN}$ 11 Gy	$(X/Fe)_{SN}$ 12 Gy	$(X/Fe)_{SN}$ 13 Gy	$(X/Fe)_{Sun}$ 13.8 Gy
Z				
1				
5				
6	7.585776	6.76083	6.606934	8.511380382
7	2.884032	2.754229	2.630268	2.13796209
8	16.2181	15.48817	14.4544	18.19700859
9				
11	0.063096	0.063096	0.06166	0.054954087
12	1.258925	1.258925	1.348963	1.258925412
13	0.087096	0.095499	0.097724	0.089125094
14	1	1.023293	1	1.023292992
15	0.007413	0.006761	0.007762	0.008128305
16	0.457088	0.47863	0.446684	0.416869383
17				
19	0.003631	0.003631	0.003715	0.003388442
20	0.075858	0.075858	0.074131	0.069183097
23	0.000282	0.000251	0.000251	0.000269153
24	0.01349	0.013804	0.01349	0.013803843
25	0.008318	0.007943	0.007943	0.00851138
26				1
27	0.00309	0.003236	0.00302	0.003090295
28	0.051286	0.052481	0.053703	0.052480746
29	0.000407	0.000427	0.000479	0.000489779
30	0.001175	0.001175	0.001202	0.001148154
33				
34				
42	3.39E-06	3.39E-06	3.39E-06	2.39883E-06
53				
74				

ORCID iDs

Vlado Valković https://orcid.org/0000-0002-3977-7410
Jasmina Obhođaš https://orcid.org/0000-0002-9347-922X

References

Adamczyk, L., Agakishiev, G., Aggarwal, M., et al. 2013, PhLB, 719, 62
Akchurin, N., Langland, J., Onel, Y., et al. 1993, PhRvD, 48, 3026
Andersson, B. G., Lazarian, A., & Vaillancourt, J. E. 2015, ARA&A, 53, 501
Asplund, M., Grevesse, N., Sauval, A. J., et al. 2009, ARA&A, 47, 481
Batty, C. J., Gilmore, R. S., & Stafford, G. H. 1963, NucPh, 45, 481
Bazilevsky, A., Alekseev, I., Aschenauer, E., et al. 2011, J. Phys. Conf. Ser., 295, 012096
Becker, S., Schneider, C., Okamura, H., et al. 2018, NatCo, 9, 163
Blackmond, D. G. 2010, Cold Spring Harb. Perspect. Biol., 11, a032540
Bolm, C., Mocci, R., Schumacher, C., et al. 2018, Angew. Chem., Int. Ed., 57, 2423
Bonner, W. A., Kavasmaneck, P. R., Martin, F. S., & Flores, J. J. 1975, Orig. Life, 6, 367
Boyd, R. N., Famiano, M., Onaka, T., & Kajino, T. 2018, ApJ, 856, 26
Bravar, A., Alekseev, I., Bunce, G., et al. 2005, Spin Dependence in Elastic Scattering in the CNI Region. Brookhaven National Laboratory. Report, BNL-75128-2005-CP
Cazaux, S., Minissake, M., Dulieu, F., et al. 2016, A&A, 585, 1
Chopra, A., & Lineweaver, C. H. 2015, Astrobiology Science Conf., ed. P. Doran, (Houston, TX: Lunar and Planetary Institute), 7328
Chopra, A., Lineweaver, C. H., Brocks, J. J., et al. 2009, 9th Australian Space Science Conf., ed. W. Short & I. Cairns, (Sydney: National Space Society of Australia), 91
Cockell, C. 2015, Astrobiology–Understanding Life in the Universe (2nd edn; New York: Wiley)
Cornish-Bowden, A., & Cárdenas, M. L. 2017, JThBi, 434, 68
Crutcher, R. M. 2012, ARA&A, 50, 29
Damer, B., & Deamer, D. 2020, AsBio, 20, 429
De Marcellus, P., Meinert, C., Michel Nuevo, M., et al. 2011, ApJL, 727, L27
Demayo, A. 1983, in Handbook of Chemistry and Physics, ed. R. C. Weast (64th edn.; Boca Raton, FL: CRC Press), F-151
Ehrenfreund, P., & Charnley, S. B. 2000, ARA&A, 38, 427
Ehrenfreund, P., Spaans, M., & Holm, N. G. 2011, RSPTA, 369, 538
Forsythe, J. G., Yu, S. S., Mamajanov, I., et al. 2015, Angew. Chem., Int. Ed., 54, 9871
Frank, F. C. 1953, Biochim. Biophys. Acta., 2, 459
Garcia, A. D., Meinert, C., Sugahara, H., et al. 2019, Life, 9, 29
Globus, N., & Blandford, R. D. 2020, ApJL, 895, L11
Greenberg, J. M. 1971, A&A, 12, 240
Greenberg, J. M. 2002, SurSc, 500, 793
Greenberg, J. M., & Li, A. 1997, in ASP Conf. Ser. 124, Grain temperatures and emission in diffuse interstellar clouds. Diffuse Infrared radiation and the IRTS, ed. H. Okuda, T. Mataumoto, & T. L. Roelling (San Francisco, CA: ASP)
Horneck, G., Klaus, D. M., & Mancinelli, R. L. 2010, MMBR, 74, 121
Ioppolo, S., Fedoseev, G., Chuang, K. J., et al. 2021, NatAs, 5, 197
Joyce, G. F., Visser, G. M., van Boeckel, C. A., et al. 1984, Natur, 310, 602
Kliewer, S. 1995, The Compact Cosmic Ray Telescope aboard the Kuiper Airborne Observatory, https://cosmic.lbl.gov/SKliewer/Index.htm
Kobayashi, C., Karakas, A. I., & Lugaro, M. 2020, ApJ, 900, 179
Kobayashi, C., Tsujimoto, T., & Nomoto, K. 2000, ApJ, 539, 26
Kolokolova, L., Koenders, C., Rosenbush, V., et al. 2015, in American Geophysical Union Fall Meeting 2015 (Washington, DC: American Geophysical Union), P41D-2089
Kolokolova, L., & Nagdimunov, L. 2014, P&SS, 100, 57
Kwok, S. 2004, Natur, 430, 985
Lamour, S., Pallmann, S., Hass, M., & Trapp, O. 2019, Life, 9, 52
Loeb, A., Batista, R. A., & Sloan, D. 2016, JCAP, 8, 40
MacDermott, A. J. 2012, in Perspective and Concepts: Biomolecular Significance of Homochirality: The Origin of Homochiral Signature of Life (Comprehensive Chirality), ed. E. M. Carreira & H. Yamamoto, Vol. 8 (Amsterdam: Elsevier), 11
McCabe, M., & Lucas, H. 2010, IJAsB, 9, 217
McGuire, B. A., & Carroll, P. B. 2016, PhT, 69, 86
Minissale, M., Dulieu, F., Cazaux, S., & Hocuk, S. 2016, A&A, 585, A24
Oba, Y., Takano, Y., Naraoka, H., et al. 2019, NatCo, 10, 4413
Obhođaš, J., Valković, V., Kollar, R., et al. 2021, AsBio, 21, 323

Okada, H., Alkseev, I., Bravar, A., et al. 2008, in AIP Conf. Proc. 980, Polarized Ion Sources, Targets and Polarimetry (Melville, NY: AIP), 370
Prelog, V. 2006, Croat Chem. Acta., 79, XLIX
Sasselov, D. D., Grotzinger, J. P., & Sutherland, J. D. 2020, Science Advanced, 6, eaax3419
Scorei, R. 2012, OLEB, 42, 3
Sharov, A. A., & Gordon, R. 2017, in Life before Earth. Habitability of the Universe Before Earth (Astrobiology: Exploring Life on Earth and Beyond), ed. P. H. Rampelotto, J Seckbach, & R. Gordon (Amsterdam: Elsevier), 265
Stolar, T., Lukin, S., Etter, M., et al. 2020, Chem. Comm., 56, 13524
Tarduno, J. A., Cottrell, R. D., Bono, R. K., et al. 2020, PNAS, 117, 2309
Valkovic, V. 2022, Origin of Life—Musings from Nuclear Physics, Astrophysics and Astrobiology (Boca Raton, F:: CRC Press)
Van Dishoeck, E. F. 2014, FaDi, 168, 9
Vogl, O. 2011, JPoSA, 49, 1299
Yin, P., Zhang, Z.-M., Lv, H., et al. 2015, NatCo, 6, 6475
Zhukovska, S., Gail, H. P., & Trieloff, M. 2008, A&A, 479, 453